DENDRITE FRAGMENTATION IN THE SHEARED MELT BY FATIGUE EROSION MECHANISM OF SEMISOLID Al-Si ALLOY (A.356.00)

M. Shahmiri

* *mshahmiri@iust.ac.ir*

Received: January 2016 **Accepted: November 2016**

School of Metallurgy and Materials Engineering, Iran University of Science and Technology, Iran.

Abstract: *Over the last few decades, there have been many mechanisms proposed to describe the formation of the non-dendritic microstructures during Semisolid Metal (SSM) processing; including dendrite fragmentation, spherical growth, cellular growth and recalescence. Dendrite fragmentation is the most popular mechanism of all these hypotheses.*

It is the purpose of the present article to examine the morphological evolution of the non-dendritic microstructures, based on models proposed by Flemings, Vogel, Cantor, and Doherty during SSM processing of the Al-Si (A356) alloy. Based on new microstructural evidences, including (1) - plastic deformation at the side arms by slip lines formation as a result of the thermal fatigue mechanism, (2) - crack formation at the root of the side arms and (3) – the interaction of a rapidly sheared hot viscous medium with these regions, i.e. erosion; it propose and hereby discuss a new mechanism called "fatigue –erosion", for dendrites fragmentation of the experimental alloy.

Optical and Scanning Electron Microscopy (SEM) with EBSD and EDS, TEM, and AFM was used for the microstructural characterizations.

Keywords: *Al-Si alloy (A356), semisolid metal (SSM) processing, melt shearing, fatigue-erosion, Dendrite fragmentation.*

1. INTRODUCTION

Semisolid metal (SSM) processing involves shearing of an alloy melt either during solidification or isothermally with a specific fraction of solid for a specific duration. It has significant advantages over conventional casting for near net shape production of industrial components. The resulting product of the melt shearing during solidification is the formation of globular solid particles in a liquid matrix. Shearing the melt in its semi solid state, usually by mechanical or electromagnetic means, has been found to be most useful in producing a non-dendritic globular morphology of primary solid phase [1, 2].

To explain the observed fine non-dendrites (spherical) particle size and morphology under melt shearing, several mechanisms have been proposed since the pioneering discovery by the MIT team [2, 3-4].

Vogel and Cantor [5] by using a boundary layer model concluded that shearing destabilises the solid-liquid interface for both low and high mobility interfaces.

Further development by the same authors for dendrite solidification under fluid flow revealed that melt shearing increases the dendrite tip velocity and decreases the tip radius [6, 7].

The apparent contradiction to the observed experimental results prompted Vogel [6] to suggest that the non-dendritic microstructure observed during melt shearing might be a result of overlapping diffusion fields of a large number of growing particles.

To explain the observed grain refinement by melt shearing, Vogel et al. [7] have proposed a dendrite arm fragmentation mechanism to account for grain multiplication.

They suggested that dendrite arms bend plastically under the shear force created by melt shearing. Plastic bending introduces large misorientation into the dendrite arms in the form of ‘geometrically necessary dislocations’. At high temperature, such dislocations rearrange themselves to form high angle grain boundaries with energy greater than twice the solid-liquid interfacial energy. This is then wetted by liquid metal, resulting in the detachment of dendrite arms.

[DOI: 10.22068/ijmse.13.4.10]

Doherty et al. [8] performed hot bending tests on single crystals of aluminium and observed the formation of high and low angle grain boundaries for a bending angle in excess of 55°.

This followed earlier suggestion by Flemings [2] and Hellawel, et, al [9-10] that secondary dendrite arms can detach at their roots because of remelting due to solute enrichment and thermosolutal convection.

The most crucial question remaining is how likely is it that low shearing can exert high bending movements to small dendrite arms in order to fracture them. Molenaar, [11-12] proposed that dendrite bending could give rise to rosette or spherical formation without any need to make mechanical effects. However, the predicted dendrite arms bending by this model has not yet been observed.

The fragmentation of dendrite arms mechanisms may be summarized as three main groups: (1) dendrite arms break off at their roots due to shear forces, (2) dendrite arms melt off at their roots, and (3) dendrite arms bend under fluid flow stresses creating boundaries within the bent dendrites followed by complete wetting of a high angle, high energy grain boundary by the liquid phase leading to eventual break–up of dendrites [13].

The third group is known as grain boundary wetting mechanisms.

Of course, in these hypotheses, dendrite fragmentation is the most popular mechanism, although this theory lacks the convincing experimental evidence.

All of the proposed mechanisms are based on indirect microstructural observation, and so far there is no report for the direct observation of the initial fragmentation stage of dendrite arms [14-16].

It is the purpose of the present article to examine the formation mechanisms of the non-dendritic microstructures, based on the models proposed by Flemings, Vogel, Cantor, and Doherty during semisolid metal processing of the Al-Si (A356) alloy.

2. EXPERIMENTAL PROCEDURE

Predetermined amounts of the alloy compositions (6.90%Si, 0.34%Mg, 0.15% Fe, 0.06%Zn, 0.17%Cu, 0.03% Pb, and 0.01%Mn, all in weight %) were melted in the graphite crucible of the SSM processing machine.

Different experimental procedures were followed in order to obtain the requested samples:

1. The melt was continuously cooled at a rate of 2.5 °C min^{-1} (used throughout the present work, unless otherwise stated) to the solidification range. After isothermal holding treatment for preset time intervals, up to 1200 seconds (corresponding to different volume fractions), the slurries were quenched in water, (unstirred alloy).
2. The same procedure as 1) was followed for production of SSM samples but after 40 seconds isothermal holding in the solidification range, the slurries were isothermally sheared (up to 1500 rpm corresponding to 1000 s^{-1}) at the predetermined temperatures for different time intervals (up to ten minutes in 30 seconds steps). They were subsequently quenched in water.
3. The same procedure as 2 was followed, but the crucibles were suddenly quenched in water while the stirring blade was still rotating inside the slurries. The liquids were sheared, up to 1000 s^{-1} for preset time intervals at a temperature range of 590 °C-610 °C, when quenched in water (called the quenching experiment).

It should be noted that alloys quenched in water are referred to as ‘WQ’, in the rest of the text, unless otherwise stated.

Several samples were mechanically ground and polished down to 1 μm by means of standard metallographic routines. The samples were etched with the modified Keller's reagent. The SEM samples for the EBSD technique were electro polished for 15 s at 37 V in 20% perchloric acid + 80% ethanol reagent as final polish .

The specimen surface was tilted 70° between the normal direction and the incident beam. This technique optimises the quality of the EBSD

[DOI: 10.22068/ijmse.13.4.10]

patterns, and the beam (20 kV accelerating voltage, $5x10^{-8}$ A beam current), when 80 nm steps are used across the specimen The solid volume fractions (f_s) were measured using an automated image analyser connected to the optical or electron microscope. The measurements were carried out on 50 random sections at different magnifications on unstirred or stirred-modified alloys [17].

Preliminary investigation of the slip bands and the dislocation arrangements on the surface of the root of the dendrites branch was made possible by using TEM and AFM on those samples, which were prepared by the ion-milling procedure. Initial surface preparation was carried out by mechanical grinding to the desired thicknesses, and subsequently the samples were ion-milled in a cold stage at 6 kV and 0.05 mA at 12° tilt for approximately 10 h. Two microscopes were used: A Philips CM20 and a JEOL 200CX, both operating at 200 kV [14, 17-19].

3. RESULTS

Typical microstructures of an unstirred alloy and the alloys produced under different semisolid processing parameters by mechanical shearing are presented in Fig.1.

A typical microstructure of an unstirred A356 alloy continuously cooled from 700°C to 600°C, isothermally held for 60 second and subsequently either WQ or cooled to room temperature, is shown. In Fig.1a, a coarse dendrite structure of the primary α–Al phase in the bright continuous matrix (quenched liquid) is shown. Fig.1b shows the microstructure of the same alloy, continuously cooled to room temperature from above the liquidus temperature. The microstructure consists of the primary α-Al phase and a eutectic two-phase mixture of α-Al+Si, which is typical of hypoeutectic Al-Si alloys.

When the same alloy was sheared with different SSM processing parameters, various non-dendrites primary solid particles substituted the dendrite structure, Fig. 2 (a, d). This figure shows the morphological evolution of dendrite in SSM slurry of A356 alloy. Alloys were sheared isothermally at predetermined temperatures - shear rates -shearing times combinations after continuously cooling from 700 °C, within the two-phase region and finally WQ.

At the beginning of the isothermal shearing, the original dendrites were quickly fragmented into small segments, Fig. 2a. With increasing isothermal shearing time, the dendrites were further broken down to smaller particles, Fig. 2 (b, c). After this, further shearing did not significantly affect the spherical morphology of A356 alloy, Fig. 2d.

Disfiguration of the primary dendrites structure during processing of the SSM alloys was captured in a rare microstructural observation in quenching experiments.

After separation of the blade from the solidified alloys in the quenching experiment (experimental procedure No.3) , the sections at

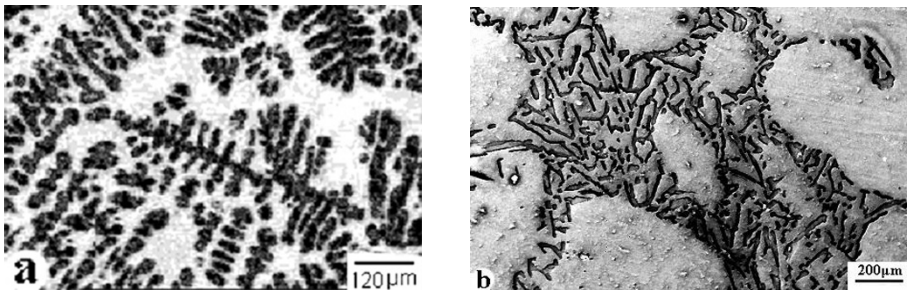

Fig.1. Light Optical microscopy image of as-solidified alloys A.356: (a)An unstirred, WQ from two- phase region, and (b) an unstirred, continuously cooled to room temperature from above the liquidus temperature.

[DOI: 10.22068/ijmse.13.4.10]

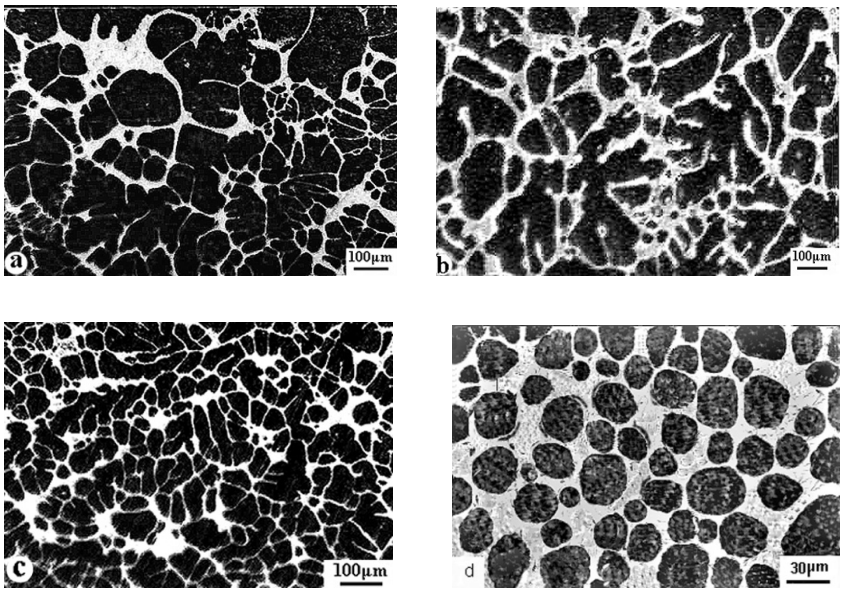

Fig. 2. Light Optical microscopy image (dark field) of the stirred alloys cooled to two-phase region: (a)Cooled at 590°C, sheared at $600S^{-1}$ for 40 seconds after isothermal holding for 40 seconds, (b) Cooled at 590°C, sheared at $600S^{-1}$ for 80 seconds after isothermal holding for 40 seconds, (c) Cooled at 590oC, sheared at $600S^{-1}$ for 120 seconds, after isothermal holding for 40 seconds, and (d) Cooled at 590°C, sheared at $700S^{-1}$ for 160 seconds, after isothermal holding for 90 seconds. All samples WQ after isothermal holding.

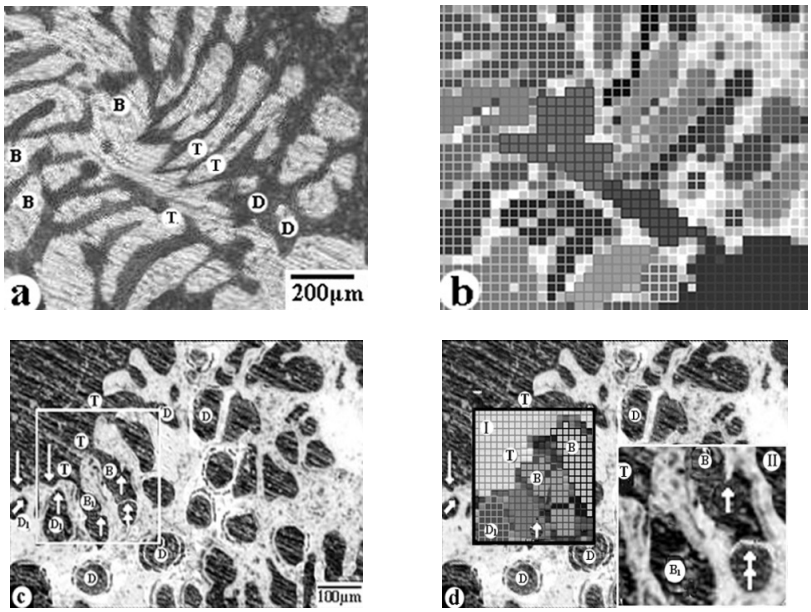

Fig. 3. SEM images of the stirred alloys cooled to two- phase region: (a) Cooled to 605°C, sheared at 700 S^{-1} for 100 seconds after isothermal holding for 120 Seconds, (b) EBSD of (a), (c) Cooled to 610°C, sheared at 1000 S^{-1} for 80 seconds after isothermal holding for 120 seconds, and (d) The same as (c), showing EBSD of the boxed area (Fig. I) and higher mag of the boxed area of (c)(Fig. II). All samples WQ after isothermal holding.

[DOI: 10.22068/ijmse.13.4.10]

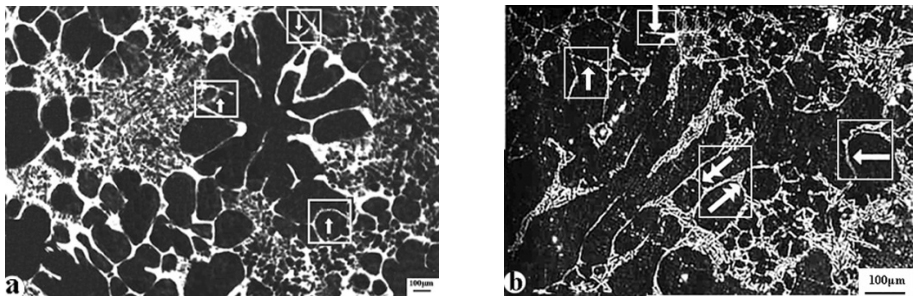

Fig. 4. SEM images of the stirred alloys cooled to two-phase region. (a) Cooled to 600 °C, isothermal sheared at 800 S^{-1} for 300 seconds after isothermal holding of 300 seconds, and (c) Similar area to (a).

different locations close to the blade surface were prepared by the standard metallographic techniques and then studied under optical and electron microscopes. In the most sections examined, a fully-grown disfigured dendritic structure was observed, as presented in Fig. 3. The disfigured dendrite was comprised of:

I. Dendritic arms thinned down at their roots, marked T in Fig. 3(a, c),
II. Bent and fractured dendritic arms marked B in Fig. 3(a, c),
III. Detached and rotated dendritic arms from the main trunk, due to the local shear forces, marked D and D1 in Fig. 3(a, c).

The EBSD images of Figs. 3a and 3c (the boxed area) revealed the crystallographic misorientation amongst the primary dendrite arms and the dendrites stem. Fig. 3b and Fig. 3d (the boxed area marked as I and II) show the relevant images.

The bent or fragmented dendrite arms revealed a misorientation of nearly 20° amongst the majority of the segments or with respect to the main dendrite stem.

A typical groove on the bent dendrite arm structure is shown in Fig. 4 (a, b).The groove

highlighted by a single arrow in these figures was characterised by a large angle, showing the state of liquid penetration/wetting. The dendrite arm, depicted by a double arrow, in Fig. 4b, indicated a complete wetting boundary.

The most pronounced effect of melt shearing on the dendrite morphological transformation obtained during the quenching experiment and Fig. 5 shows the quenched microstructure.

In this figure, a disfigured dendrite comprising

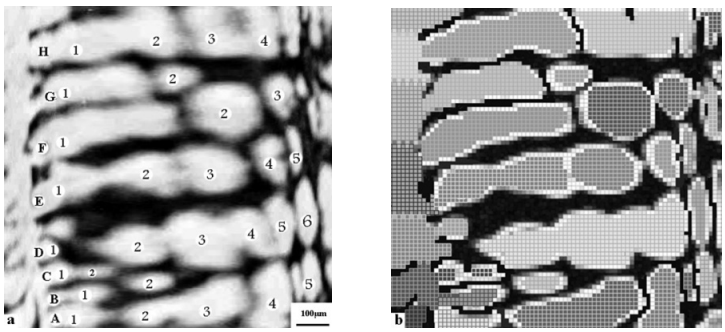

Fig. 5. SEM images of the stirred alloys cooled to two-phase region: (a) Cooled to 610 °C, sheared at 1000 S^{-1} for 20 seconds, after isothermal holding for 80 sec, WQ and (b) COM of (a).

[DOI: 10.22068/ijmse.13.4.10]

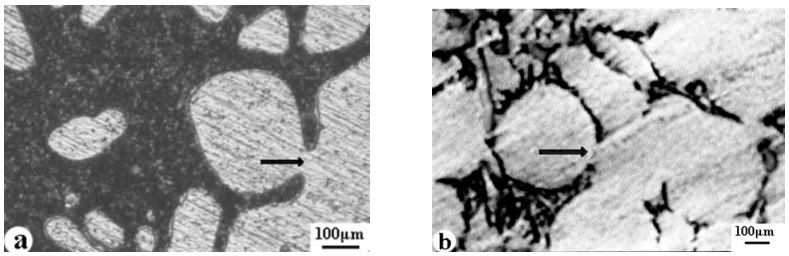

Fig. 6. SEM images of necking dendrites arms due to shearing: (a) Section of Fig. 3, and (b) Section of Fig.4.

of the primary dendrite stem (on the left) and the dendrite branches (on the right) is visible. The following phenomena are noticeable:

A. Necking developed in different sections of a dendrite branch, e.g. A (1-2), A (3-4), D (2-3), E (1-2), and E (2-3), etc, similar to the necking during a tensile test,
B. Some segments of the dendrite branches are detached from the rest, e.g. D (1-2), C (1-2), and E (1-2), etc, and
C. The radius of the curvature at the roots of a dendrite branch reduced, e.g. at G, E and F. This could well be the effect of liquid penetration in these regions due to the melt shearing. Fig. 5b shows the EBSD image of the Fig. 5a, in which the orientation changes along the individual branches of a disfigured dendrite (either necked or detached), is visible. It appears that, when the misorientation angle along the dendrite branches exceeded a critical value (e.g.20° between F1-F2) the detaching mechanism(s) proceeds.

Fig. 6 provides further microstructural support for the reduction of the radius of the curvature at the root of a dendrite branch during SSM processing of the experimental alloy. It seems that, while the growth of a dendrite branch segment is continued towards the remaining liquid, further reduction of the root radius takes place as a result of liquid penetration. This mechanism continues to proceed until the dendrites arm is detached from the dendrites stem. The particles D1 in Fig. 3c can be treated the same as the dendrite branch segment shown in Fig. 6, but after detachment.

To provide further microstructural clarifications, AFM and TEM investigations were carried out. Fig. 7a shows an AFM image of the root surface (similar to the one denoted by arrow in Fig. 6), which consists of surface steps (slip bands) with regular spacing of a few microns

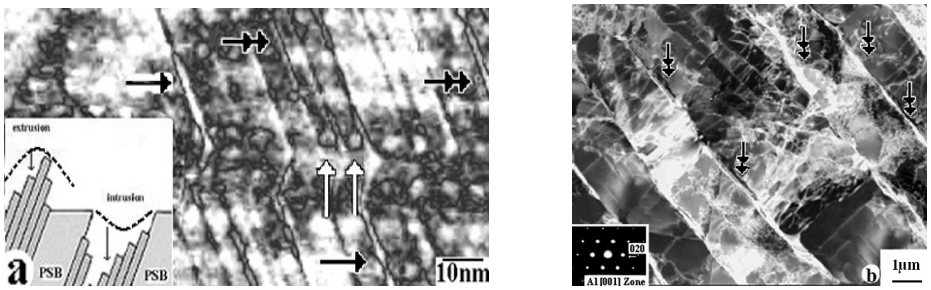

Fig. 7. Microstructures of the necked regions of dendrites arms, similar to the boxed area of Fig. 3(d): AFM of slip lines, and (b) TEM image of slip lines and Selected Area Diffraction Patterns.

[DOI: 10.22068/ijmse.13.4.10]

running from the upper left to the lower right-hand side of the micrograph. These slip bands indicate that they were formed during SSM processing of the alloys under the shear stress action.

Two distinct features of the liquid penetration or the wetting of the dendrite branch root by the shearing melt is revealed in Fig. 7a. The wetting of the root area is shown in the form of a thin layer (single arrows, black) and the other is in the form of a sphere (twin arrow, white). At this stage, it appears that the wetting of the dendrites root surface depends on the nature of the persistent slip bands characteristics, i.e. intrusion or extrusion.

Preliminary TEM investigations revealed the dislocation structures and the sub-boundaries within the slip bands (Fig. 7b). In both TEM and AFM images, the micro cracks formed during melt shearing is observed (double arrows, black). The slip bands parallel to $<0\overline{11}>$ direction are considered to have formed by the slip system of $a/2 <0\overline{11}> \{111\}$ [13]. This indicates that the slip bands correspond to 45o shear type according to Shahmiri et al [19-20].

4. DISCUSSION

The present results showed that melt shearing during solidification within the two-phase region, transferred the dendritic structure of the primary α-Al solid phase to a rosette-like and eventually spherical morphology in a semisolid processed Al-Si (A356) alloy. This process produced grain refinement and greater structural uniformity in the final cast structure.

The fragmentation process occurs very rapidly, after shearing the melt and completes within the first few seconds. The spheroidisation mechanism of the dendrite fragments is a much slower process, (Figs.1-2).

The results showed that usually 60 seconds of shearing was sufficient for dendrite fragmentation in semisolid slurries by mechanical stirring. The dendrite arms bent (Fig. 3(a-c) during shearing and are then wetted by liquid alloy in a semisolid slurry to form large angle grooves across the sections, resulting in the formation of fine and spherical primary particles [17, 26-27].The results imply that the formation of the primary particles can be attributed to the penetration of the liquid alloy along the grain boundaries (Figs. 3-4), in the bent dendrite arms formed during shearing semisolid slurry. The grain boundaries are formed by recovery of the "geometrically necessary dislocations" generated by plastic bending of dendrite arms under viscous force [21-22].

Liquid alloy would subsequently wet the grain boundary, resulting in the dendrite arm detachment. According to Ji [19-20] in this process, there are at least two stages of formation of grain boundaries in the dendrite arms and wetting along the grain boundaries.

Under this condition in the semisolid slurry, all the detached dendrite segments (acting as new nuclei) grow very quickly to a size corresponding to the preset solid volume fraction dictated by the SSM processing temperature. Due to the uniformity of both temperature and composition fields within the liquid, the growth conditions for all the particles are nearly identical and they tend to consequently develop into globular particles of similar size.

According to the Gibbs-Thomson effect, any possible size difference between particles will be reduced, due to the enhanced mass transport through the remaining liquid phase. Therefore, shear forces ensures spherical particle morphology during the primary solidification [21].

The microstructural evolution described by previous studies, such as Biro, and Legoretta et al [21 22] and Doherty el at [5-9] that support dendrite fragmentation mechanism of sheared melt, have been observed in more detail in the present study.

Almost all of the previous studies [23-25] believe that the mechanical stresses are unable to directly bend the dendrite arms plastically and fracture them. In other words, there must be a mechanism of dendrite fragmentation that can function, even under low stress conditions.

The slip bands and micro cracks on the skin at the root of the dendrite arms (Fig. 7) seem to be the most important micro structural features observed in the present investigation to reveal the nature of a mechanism, which we call "fatigue-erosion" which is explained below.

It is well known that alloys in high temperature

[DOI: 10.22068/ijmse.13.4.10]

fatigue tests fracture under loads much smaller than their yield strength. Microcracks initiate on the surface where stress concentration occurs, and tend to propagate with the help of continuous stress provided by melt shearing [25-27]. Another characteristic is the creation and propagation of the slip bands (extrusion and intrusion) within several cycles of deformation in high temperature fatigue.

A similar situation can be adopted for the dendrite arms during melt shearing of the experimental alloy [16]. In semisolid slurries, the dendrite arms are in continuous cyclic collision with the hot fluid flow and with each other. It is difficult to substantiate the true nature of the fluid flow pattern due to shearing and the high shearing temperature of the SSM processed alloy. The following uncertainties should be taken into account:

- Shear and compression components, individually or superimposed
- Intermediate flow due to the primary particles rotation.
- Microscopic flow due to the angular or surface roughness of primary particles.

Whatever the true nature of the fluid pattern might be, it is certain that a cyclic deformation is expected to act on the dendrite arms. In other words, the initially formed dendrite arms are clamped to the dendrite stem and free at the other end, behaving like a beam during the initial stages of shearing. A regular cyclic stress develops and is expected to act on the dendrite arms, especially the clamped end (similar to the root of the arms).Therefore it is logical to associate the gradual detachment of the dendrite arms with high temperature fatigue mechanism. The slip bands and the micro cracks observed on the skin at the root of the dendrite arms are due to the dendrite arms continuously bending during shearing. According to Lee [25], in this process the dislocation density is increased for the sheared dendrite arms and sub grain boundaries can form after dislocation migration under shearing.

The radii of the curvature of the slip band intrusion and extrusion are very small. This will increase the interfacial energy and decrease the local melting point in these stress regions. The slip band intrusion and extrusion on the skin of the root will decrease the melting point of the solid surface and cause erosion. Subsequently, a new and more curved surface is formed at the root of the dendrite arms. This is true when the erosion rate of the surface of the root will gradually be eroded and finally ruptured.

The arms often show constricted growth where they attach to the primary trunk. This is as the result of growing through the enriched layer and thermosolutal convection due to shear. Consequently, the base of a secondary dendrite arm becomes much narrower and hence it deforms more easily than other parts.

At the same time, the sheared melt collides cyclically with the dendrite arms, and gradually erodes the roots of the dendrite arm and eventually detaches them. Similar to high temperature fatigue, the erosion mechanism will accelerate after it begins, due to stress concentration, as the diameter of the neck region decreases. As erosion continues, the diameters of the eroded roots will finally be so thin that plastic bending is possible [16]. At the final stage of dendrite fragmentation, the dendrite arm will be detached by the mechanism of recrystallization followed by rapid liquid penetration.

The cracking is presumed to expose fresh surfaces, deeper into the dendrite arms. Subsequently, a fresh eroded layer is formed and that undergoes additional stress erosion, and so on.

The process repeats until a critical crack size is reached and surface layer of the arms fractures. Thus, the fatigue damage occurs only in the surface layer, and the observed slip bands are the result of such a mechanism [16, 19-20].

Based on the present results, it is reasonable to attribute a fatigue erosion mechanism to the dendrite arm fragmentation. The mechanical shearing can plastically bend the initial dendrites arms (by fatigue mechanism) and resulting in the formation of grain boundaries in the bent dendrite arms. The liquid alloy in sheared slurry could subsequently wet and penetrate the grain boundaries (by erosion mechanism), which eventually breakdown the dendrite into small

[DOI: 10.22068/ijmse.13.4.10]

segments [27-31].

4. CONCLUSIONS

1. Mechanical shearing the partially solidified alloy(even at low shear rates) can result in the fragmentation of the dendritic structure. The fragments of the dendrite arms produced a fine spherical structure, due to the growth in the uniformed thermo-solutal fields.
2. Stress concentration at the roots of the dendrite arms is so great that plastic bending easily occurs (by fatigue mechanism).
3. The slip bands intrusions and extrusions on the skin of the dendrite arm root will decrease the melting point of the solid surface and cause erosion.
4. The high temperature fatigue-erosion followed by hot liquid alloy penetration into the grooves along grain boundaries is the governing mechanism to fragment the dendrite arms into small segments.

REFERENCES

1. Fan, Z., “Semisolid metal processing”, International Materials Reviews, 2002, Vol. 47, no. 2, 1-37.
2. Flemings, M. C., "Behavior of metal alloys in the semisolid state", Metallurgical Transactions A, 1991, Vol. 22, no. 5, 957-981.
3. Kirkwood, D. H., "Semisolid metal processing', International Materials Reviews, 1994, Vol. 39, no. 5, 173-189.
4. Atkinson, H. V., "Modeling in semisolid processing of metallic alloys, Progress in Materials Science 2005, Vol.50, 341-412.
5. Vogel, A. and Cantor, B., "Stability of a spherical particle growing from the stirred melt, Journal of Crystal Growth, 1977, Vol. 37, 309-316.
6. Vogel, A, "PhD thesis," University of Sussex, UK, 1977.
7. Vogel, A., Doherty, R. D. and Cantor, B., "Solidification and Casting of Metals" The Metals Society, London, 1979, 518-525.
8. Doherty, R. D., Lee, H. I. and Feest, E. A., "Microstructure of stircasst metals" Materials science and engineering A, 1984, Vol.65, No.1, 181-189.
9. Hellawell, A., "Grain evaluation in conventional and Rheocasting, " Proceedings of the fourth international conference on semisolid processing of alloys and composites, Sheffield, UK, 1996, 40-48.
10. Hellawel, T., Stjohn D. H. and Steiberg, T., “The shear behavior of partially solidified Al-Si-Cu alloys,” Materials science and engineering, 2000, Vol. A286, 18-29.
11. Molenaar, J. M. M., Salemans, F. W. H. C. and Katgerman, L., "The structure of stir sat Al-6Cu, Journal of Materials Science, 1985, Vol.20, 4335- 4344.
12. Molenaar, J. M. M, Katgerman, L and Kool, W, H., "On the formation of stircasst structure," Journal of Materials Science, 1986, Vol 21, No 2, 389-394.
13. Apaydin, N, Prabhakar, K and Doherty, R., "Special grain boundaries in Rheocast Al-Mg, 12 "Materials science and engineering Journal. 1980, Vol.46, No 2, 145-150.
14. Seijiro M., Yasunori H. and Ken.Ichiro M., “Application of resistance heating technique to mushy state forming of aluminum alloy”, Journal of materials processing technology, 2002, Vol.125-126, 477–482.
15 Barabazon, D, Browne, D. J, Carr A. J., “Mechanical Stir casting of aluminum alloy from the mushy state: process, microstructure and mechanical properties.” Materials science and engineering A, 2002, Vol, 236. 370–381.
16. Lee, B. S., Joe D. H. and Kim M. H., “Extrusion behavior of Al-Cu Alloy in the semi-solid state”, Materials science and engineering, 2005, Vol. A 402, 170–176.
17. Ghalambaz, M. and Shahmiri, M.," Neural network modeling of the effect of cooling slope casting parameters on particle size of primary silicon crystals of semisolid cast ingots Al-20Si (wt.%)," Iranian Journal of materials science and technology, 2008, Vol 5 no 3, 25-32 (In English).
18. Ghalambaz, M. and Shahmiri, M., "Neural network prediction on the effect of semisolid metal processing parameters on particles and shape factor of primary alpha-Al Aluminum alloy A356.0," Iranian Journal of materials science & technology, 2007, Vol. 4, no 1 & 241-

[DOI: 10.22068/ijmse.13.4.10]

47 (In English).
19. Shahmiri, M., Hosseini, S. and Kanani, N., "Stir-Modification of the Eutectic Silicon Crystals of A356.0 Aluminum Alloy by Mechanical Stirring", 2005, Metall. 59, Vol.1-2, 557-562.
20. Shahmiri, M. and Kanani, N., "Stir-modification of Primary Si Crystals in Semisolid Metal Processed Hypereutectic Al-Si (20 wt.%) Alloy by Fatigue-erosion Mechanism". , 2008, Mettal, 62,Vol.1-2. 548-555.
21. Birol Y., "Cooling slope casting and thixoforming of hypereutectic A390 alloy", Journal of Materials Processing Technology, 2007, Vol. 207, 200-203.
22. Birol, Y., "A357 thixoforming feedstock produced by cooling slope casting," Journal of 13 Materials Processing Technology, 2007, Vol.186, no. 1–3, 94–101.
23. Haga, T. and Suzuki, S., "Casting of aluminum alloy ingots for thixoforming using a cooling slope", Journal of Materials Processing Technology,2001, Vol.118, 169-172.
24. Haga, T. and Kapranos, P., "Simple rheocasting processes", Journal of Materials Processing Technology, 2002, Vol. 130-131, 594-598.
25. Lee, H. I., Lee, J. I. and Kim, M. I.," Proc 3rd Inter. Conf. Semisolid Processing of Alloys & Composites, Ind. Sci. Uni. of Tokyo. 1994, Jan.13-15, 281-289.
26. Dhindaw, B. K., Kumar, A, Alkarkhi N. C. and Fredricksson, H., "Microstructure development and solute redistribution in aluminum alloys under low and moderate shear rates during rheo-processing", Material Science and Engineering, 2005, Vol. A, 413-414, 156-164.
27. Legoretta E. C., Atkinson H. V. and Jones, H., "Cooling Slope Casting to Obtain Thixotropic Feedstock I: Observations with a Transparent Analogue", Journal of Materials Science Aug, 2008, Vol. 43 Issue 16, 5448–5455.
28. Legoretta E. C., Atkinson H. V. and Jones, H., "Cooling slope casting to obtain thixotropic feedstock II: observations with A356 alloy," Journal of Materials Science, 2008, Vol 43, 5456-5469.
29. Lima Filho, D. P. and Yamasaki, I., "Evaluation of strip rolling directly from the semisolid state", Solid State Phenomena, 2006, Vol. 116-17, 433-436.
30. Kido, F. and Motegi, T., "Semisolid continuous casting of AS41B magnesium alloy using inclined cooling plate", International journal of Cast Metals Research, 2008, Vol. 21, no. 1-4, 105-108.
31. Guan, R. G., Cao, F. R., Chen, L. Q., Li, J. P. and Wang, C., "Dynamical solidification behaviors and microstructural evolution during vibration wavelike sloping plate process", Journal of Materials Processing Technology, 2009, Vol.209, 2592-2601.

[DOI: 10.22068/ijmse.13.4.10]